

# Design of a novel transverse flux machine

G. Kastinger

Robert Bosch GmbH

Division: Body Electronics, Engineering Advanced Development

P.O.Box 1163, D-77813 Bühl, Germany

phone: +49 7223 82 2833 – fax: +49 7223 82 7833 – e-mail: Guenter.Kastinger@de.bosch.com

**Abstract** — This paper describes the design of a novel permanent magnet excited transverse flux machine. The rotor shares the same construction as hybrid stepping motors and has a permanent magnet ring, magnetised axially. The ring-shaped stator winding is surrounded by U-shaped elements and additional core-back elements. This paper focuses on the design of such machines by 3D-FEA and their mechanical construction. Simulations compare well with experimental results.

## 1. Introduction

The transverse flux technology is over one hundred years old and was first described by W. M. Morday, who applied for the first patent in 1895. Today several universities are researching this field. The most well known work has been arrived at RWTH Aachen [3], TU Braunschweig [8] and the University of Newcastle Upon Tyne [7]. The transverse flux machine is generally considered as difficult to manufacture and too complicated and thus as too expensive. This prevents most companies from using this motor concept.

## 2. Machine Design

The principle of the permanent magnet excited transverse flux machine, in its simplest form, is presented in Fig.1.

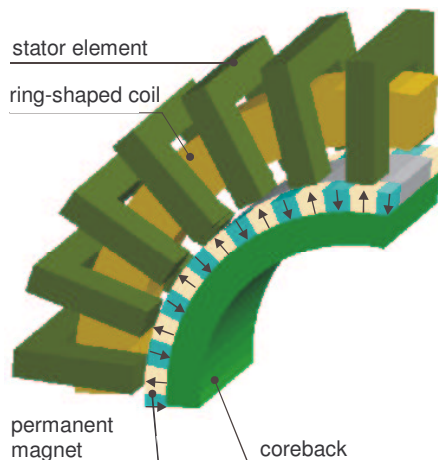


Fig.1. Permanent magnet excited transverse flux machine

Compared to classical motor concepts, a completely different mechanical structure is necessary. The typical

three-dimensional structure does not normally allow the ferromagnetic elements to be laminated and the necessary small pole pitch often demands a large number of individual parts. Moreover, problems with the realisation of the multipolar magnetisation can occur. For arrangements with relatively small permanent magnet height, the magnetisation of a multipolar permanent magnet ring is possible. If this height becomes excessive, then the rotor can be arranged using single magnets. This however increases costs further.

Hybrid stepping motors are designed, using a permanent magnet ring magnetised axially, as presented in Fig.2.

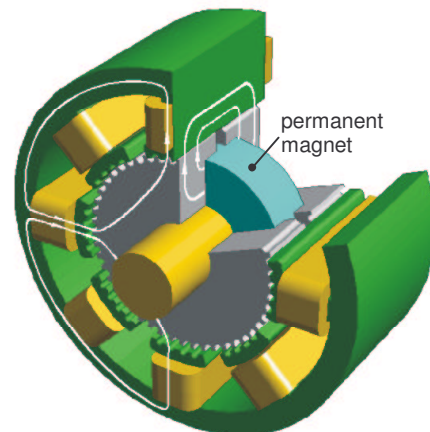


Fig.2. Hybrid stepping motor

The goal is now to implement this rotor arrangement into a transverse flux machine [2][6]. In order to achieve this, the stator arrangement of a transverse flux machine with additional core-back elements must be used [1]. A new motor arrangement is obtained, illustrated in Fig.3.

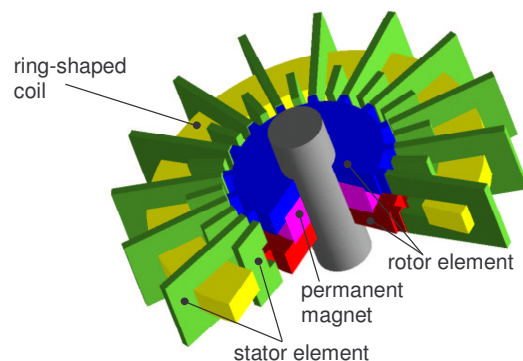


Fig.3. Arrangement of the new transverse flux motor

The stator of this new motor concept consists of laminated U-shaped stator elements and a concentrated ring-shaped coil. The rotor is made of laminated rotor elements and an axially magnetised permanent magnet ring. These laminated rotor elements form, at the circumference, a tooth-slot geometry. As for hybrid stepping motors, the ferromagnetic rotor has a recess, where the permanent magnet ring is embedded. The new motor design has the following advantages:

- simple magnetisation of the rotor with high pole-number
- only one permanent magnet per phase is required
- easily manufactured ring-shaped coil
- large current density and thus large force densities can be expected
- both rotor and stator elements are laminated
- both rotor magnet and stator coil are concentric
- good cooling possibilities

If two equivalent phases are shifted by  $90^\circ$  electrical, then a motor with a defined start is possible.

This motor concept combines items of a hybrid stepping motor with those of a transverse flux motor with additional core-back elements.

### 3. Constructional Design

The constructional design of the magnetically active elements is presented in Fig.4.

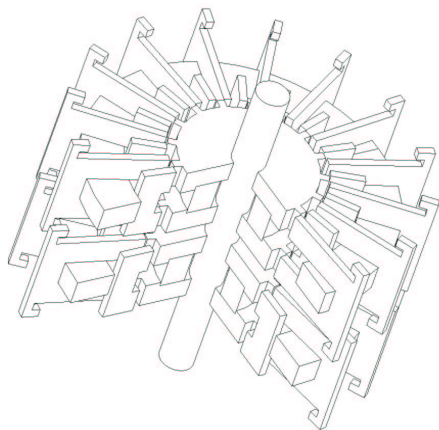


Fig.4. Constructional design

The laminated stator elements are held and positioned by a press-fit in a bobbin coil. The carrier part does not consist of one solid piece. One phase is built on two half-shells (Fig.5).

The carrier parts have recesses on the outer periphery, according to the coil form, in which, the circular coil of a phase is accommodated.

The stator elements have not only a magnetic function but also add to the mechanical compactness of the modular building method by clamping together and centring each phase. That is, the stator elements serve also for holding together and positioning the two half shells both in the axial direction, the radial direction and at the circumference. The grouping of the stator elements around

a certain angle is necessary for arrangements with multiple phases, if the laminated rotor teeth are aligned axially. Through appropriate shaping of the connection of the bobbin coil to the stator elements, a centring of the internal and external stator elements is ensured, thus centring the entire stator to the rotor.

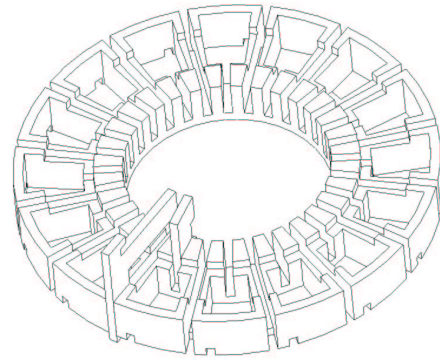


Fig.5. Carrier part (one half-shell)

With machines having multiple phases one can also implement, easily and exactly, the angular grouping of the individual phases on the rotor. Here, the stator elements are preferably in the axial direction mechanically connected or are from one stamping.

All positioning and support functions can be executed in one process step.

The end plates can be realised in different ways. For example, a half-shell can be constructed with an integrated end plate. If identical half-shells are necessary for reasons of mass production, then end plates must be attached externally.

Only one module can be used if, for example, a flat motor construction is required. However, with this arrangement, starting is not guaranteed without an appropriate modification of the one-phase arrangement. A solution for this is presented in Fig.6.



Fig.6. Principal design of a two-phase arrangement with only one module

The stator elements are divided into two groups, distributed at the circumference, each of which implement one phase. The two groups of both phases have again an angular shift of  $90^\circ$  electrical.

The coil is no longer circular and is seen to be of an unfavourable shape. In addition, the number of stator elements is reduced by the end winding and at least twice as much copper will be required with regard to the torque which can be reached.

With this two-phase arrangement a defined start in a certain direction is ensured without modification of the operational principle.

#### 4. 3D-FEA

By means of 3D-FEA, the operation of a two phase model was simulated (Fig.7).



Fig.7. Prototype

An analytical calculation or 2D-FEA is sufficient to compute approximate torques and to analyse field variations [4][5]. However, a 3-dimensional model must be used in order to obtain accurate results. Therefore, a three-dimensional finite element model was constructed by means of the FEA program Maxwell3D™. The geometry of the 3D-model is illustrated in Fig.3. Fig.8 shows the mesh of this model without the coil.

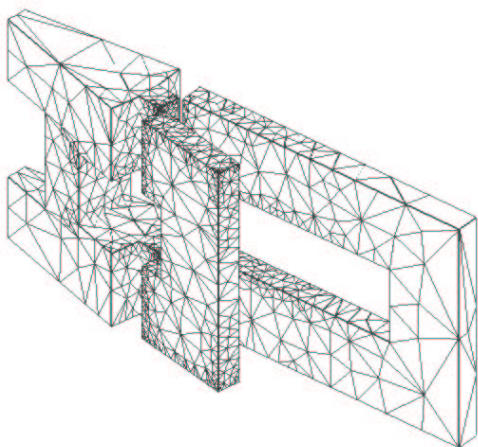


Fig.8. Meshed finite-element model of the motor

Since the motor consists of a series of identical modules which are not magnetically coupled, only one of these modules must be calculated. In Fig.9, the flux density distribution inside a module is displayed.

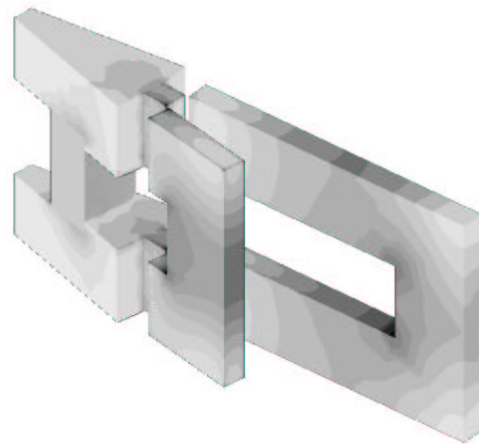


Fig.9. Flux density distribution by means of 3D-FEA

Fig.10 shows the results of the total torque versus position for different ampere-turns. The air gap length is 0.3 mm.

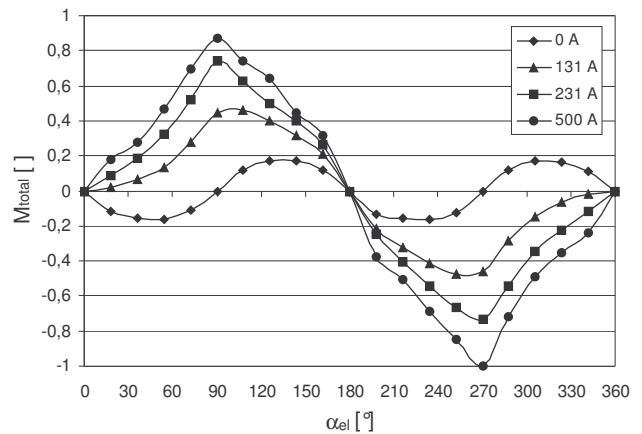


Fig.10. Total torque (normalised) versus angle and ampere-turns

The asymmetrical profile of the torque waveform arises as a result of the sum of torques produced by the permanent magnets and by the armature current. With higher ampere-turns no linear rise of the torque is recognisable. This is due to the saturation of the iron material.

For different numbers of poles, the width of the stator elements must be adapted to the pole pitch (Fig.11).

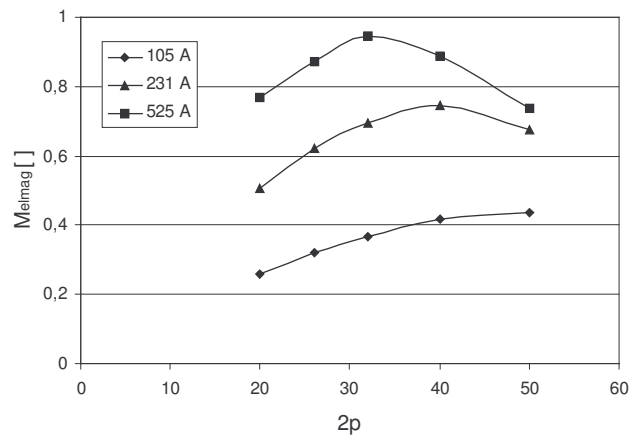


Fig.11. Electromagnetic torque (normalised) versus number of poles and ampere-turns

In the calculation the air gap is kept constant ( $\delta=0.3$  mm). The flux leakage in the air gap increases with higher numbers of poles. This effect becomes more pronounced with increasing ampere-turns (Fig.11). For the following calculations the number of poles is 32.

Fig.12 shows the influence of the rotor tooth height on the torque waveform. The ampere-turns is 231 A and the air gap length is 0.3 mm.

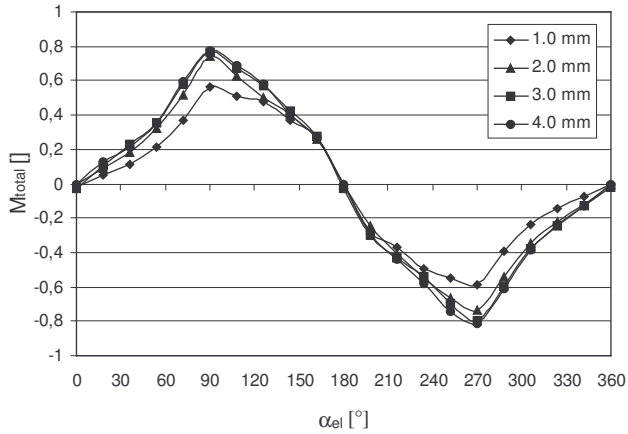


Fig.12. Total torque (normalised) versus angle and rotor tooth height

Increasing the height of the teeth over 2.0 mm leads to no considerable increase of torque.

The air gap should be as small as possible, in order to produce a high torque (Fig.13).

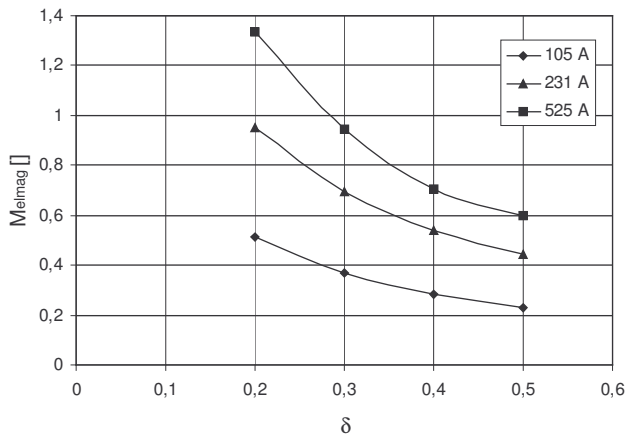


Fig.13. Electromagnetic torque (normalised) versus air gap length and ampere-turns

However, the minimal air gap length is fixed due to manufacturing tolerances. The calculation is therefore limited to air gaps from 0.2 up to 0.5 mm. With higher ampere-turns the torque characteristics deviate ever more from a linear rise. The reasons for this are flux leakage and saturation, which also affect unfavourably the torque waveform.

A variation of the rotor tooth length is presented in Fig.14, whereby the total torque is calculated over a complete electrical angle. The ampere-turns is 231 A and the air gap length is 0.3 mm.

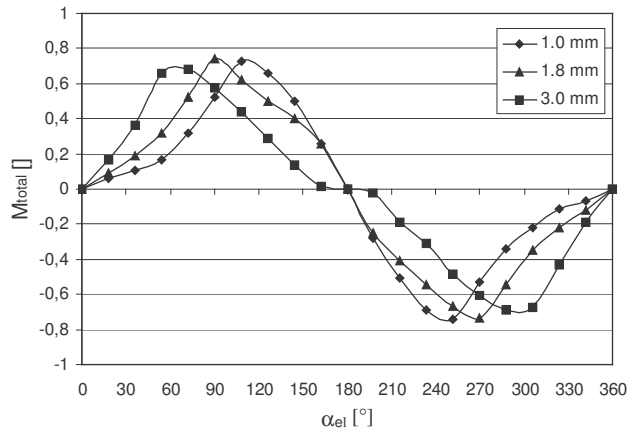


Fig.14. Total torque (normalised) versus angle and rotor tooth length

If necessary both the width of the large and small stator elements can be varied for a given number of poles. The thickness of the stator elements influences the cross section for the magnetic flux and thus the saturation of the iron. For the given arrangement, with appropriate ampere-turns, no large influence is detected by the variation of the thickness of the stator elements (Fig.15).

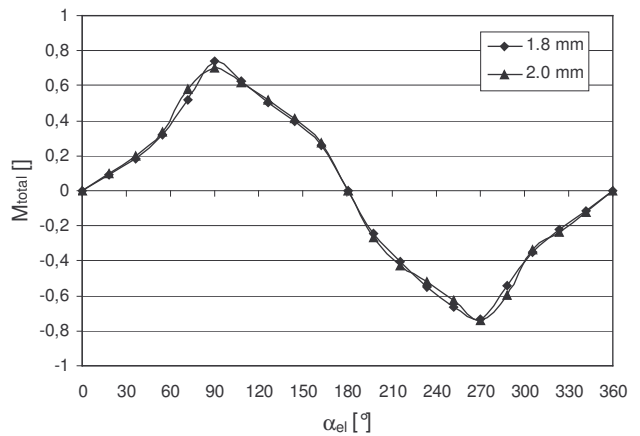


Fig.15. Total torque (normalised) versus angle and stator element thickness

## 5. Numerical simulation

The dynamic behaviour of an electrical motor can be described by a differential equation system, consisting of an electrical and a mechanical differential equation. The mechanical motion equation is shown below:

$$J \frac{d\omega}{dt} = M_{el}(\alpha, i_1, i_2) - M_{friction}(\omega) - M_{load}(t) \quad (1)$$

The electromagnetic part of the motor can be represented by the voltage equation and the induced voltage as follows:

$$U = I_{coil}R + U_{ind} \quad (2)$$

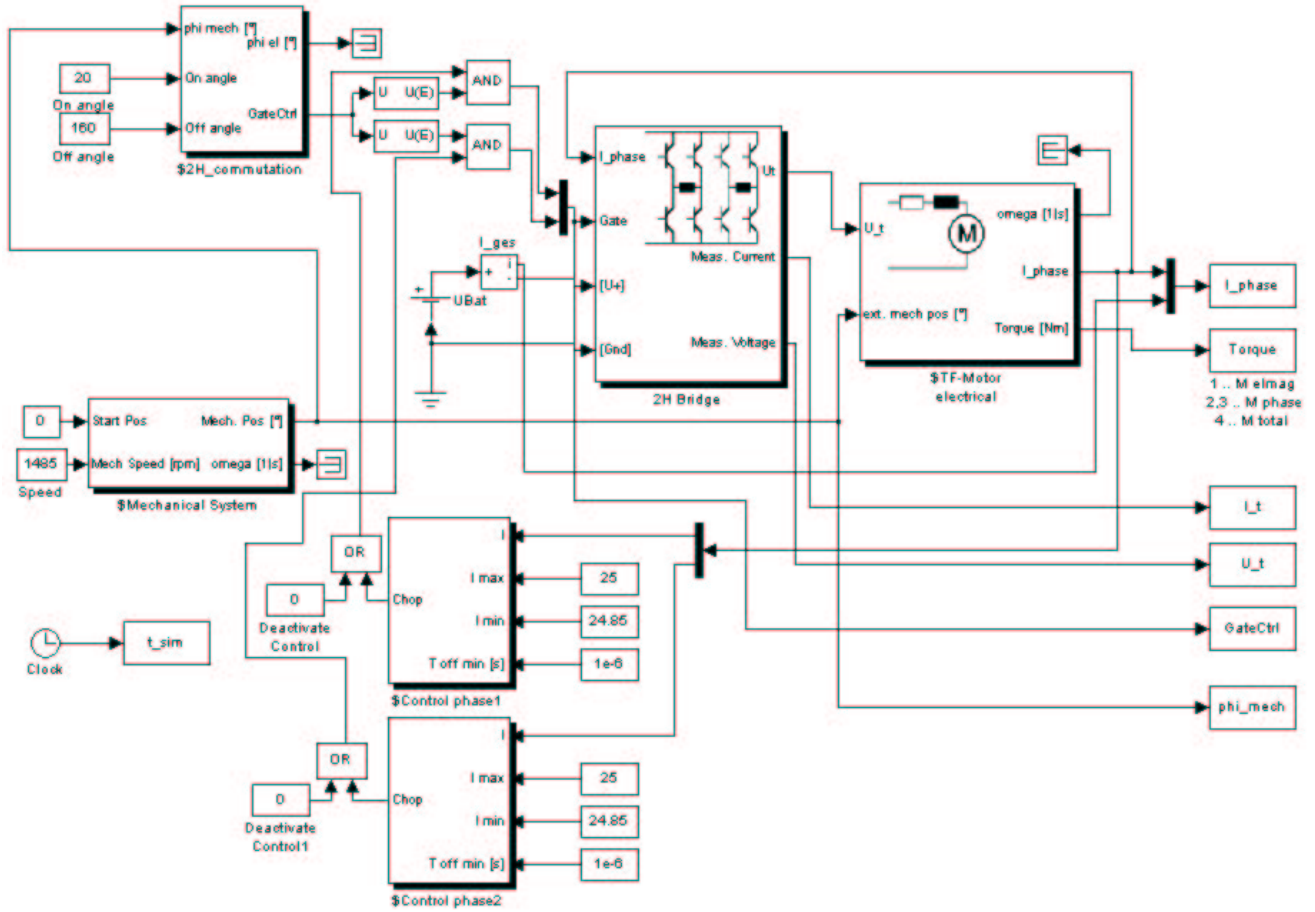


Fig.16. Simulink-model

$$U_{ind} = \frac{d\psi}{dt} \quad (3)$$

The differential equation system can be given in a form, which can be entered directly into a numerical calculation program, e.g. Matlab/Simulink™.

$$\begin{pmatrix} u_1 \\ u_2 \end{pmatrix} = \begin{pmatrix} i_1 R + \frac{d\psi_1(\alpha, i_1, i_2)}{dt} \\ i_2 R + \frac{d\psi_2(\alpha, i_1, i_2)}{dt} \end{pmatrix} \quad (4)$$

$$\begin{aligned} \dot{x} &= f(x, u) \\ y &= g(x, u) \end{aligned} \quad (8)$$

The pertinent model is shown in Fig.16.

Therefore, the differential equation system is 4<sup>th</sup> order:

$$\frac{d\alpha}{dt} = \omega \quad (5)$$

$$\frac{d\omega}{dt} = \frac{1}{J} (M_{el}(\alpha, i_1, i_2) - M_{friction}(\omega) - M_{load}(t)) \quad (6)$$

$$\begin{pmatrix} \frac{di_1}{dt} \\ \frac{di_2}{dt} \end{pmatrix} = \begin{pmatrix} \frac{\partial \psi_1}{\partial i_1} & \frac{\partial \psi_1}{\partial i_2} \\ \frac{\partial \psi_2}{\partial i_1} & \frac{\partial \psi_2}{\partial i_2} \end{pmatrix}^{-1} \begin{pmatrix} u_1 - i_1 R - \frac{d\psi_1}{d\alpha} \omega \\ u_2 - i_2 R - \frac{d\psi_2}{d\alpha} \omega \end{pmatrix} \quad (7)$$

## 6. Measurements

### A. Static torque curve

Fig.17 and Fig.18 show a comparison of measured and 3D-FEA-computed static total torque and cogging torque. The ampere-turns is 131 A and the air gap length is 0.35 mm.

The comparison of the measured and 3D-FEA-computed results is seen to be good. Small differences exist due to, for example, inaccuracies of modelling the material characteristics, etc..

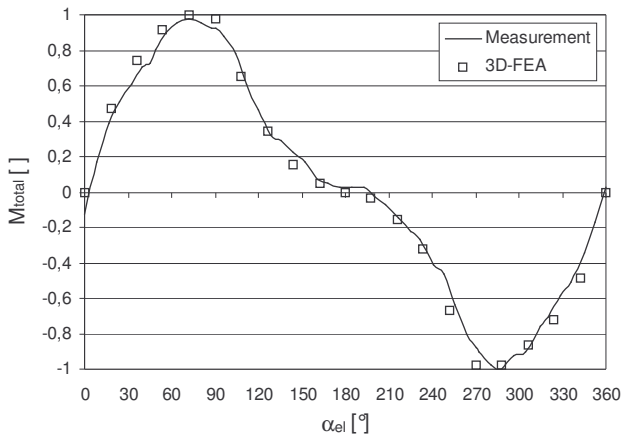


Fig.17. Total torque (normalised) versus angle

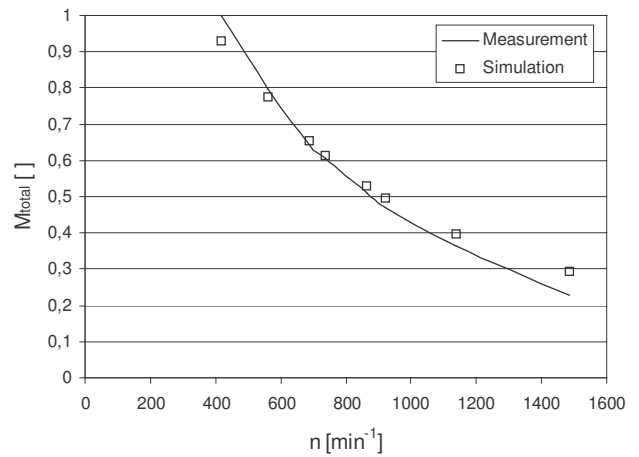


Fig.20. Torque-speed characteristic  $M=f(n)$

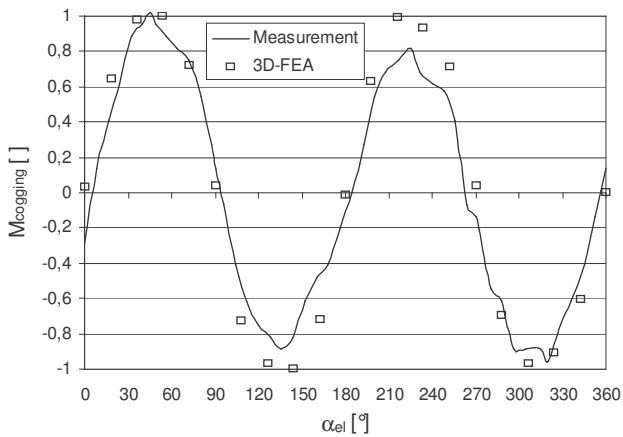


Fig.18. Cogging torque (normalised) versus angle

### B. Torque-speed characteristic

For operation of the transverse flux motor, a universal frequency converter is used (Fig.19).

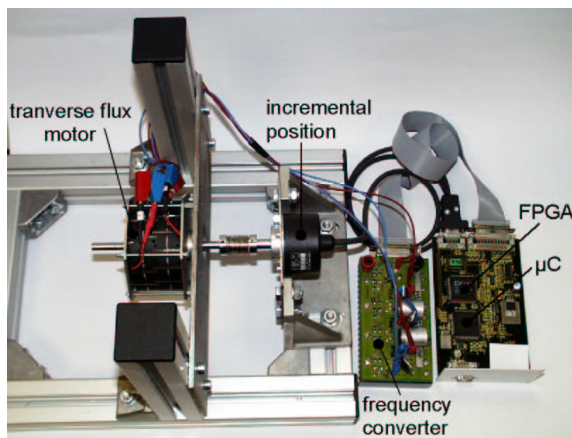


Fig.19. Experimental set-up

Using the mathematical model, described in section 5, the torque-speed characteristic can be determined. Fig.20 shows both the calculated and measured characteristics. The agreement is seen to be good.

## References

- [1] Bork M., Henneberger G.: "New transverse flux motor concept for direct drive of electric vehicle", ISATA, Florenz, 1997.
- [2] Detela A.: "Hybrid synchronous machine with transverse magnetic flux", Patent EP0544200, 1993.
- [3] Henneberger G., Bork M.: „Development of a new Transverse Flux Motor“, IEE, London, 1997.
- [4] Kastinger G.: "Analysis of Torque Computation of a Toroid-Coil-Motor by Finite Element Method“, PCIM'98 Intelligent Motion, 1998.
- [5] Kastinger G.: "Performance and Design of a Toroid-Coil-Motor with Permanent Magnets“, speedam'98, Sorrento, 1998.
- [6] Kastinger G.: "Beiträge zu Ringspulenkleinantrieben", Thesis, Johannes Kepler University Linz, 2001.
- [7] Maddison C.P., Mecrow B.C. and Jack A.G.: "Claw Pole Geometries for High Performance Transverse Flux Machines", ICEM, Istanbul, 1998.
- [8] Weh H.: "Ten years of research in the field of high force density-transverse flux machines“, speedam'96, Capri, 1996.